Bulgarian Journal of Physics vol. **XX** (20XX) 1–21

Constructing Phase-Equivalent Potential Using Supersymmetric Approach

M. Majumder, **D. Naik**, **B. Swain**, **U. Laha***
Department of Physics, National Institute of Technology,
Jamshedpur, 831014, India
*Corresponding author Email: ujjwal.laha@gmail.com

Received *25 August 2024*

Abstract. In this work, we construct a series of energy-dependent phase equivalent potentials to a combined, nuclear and electromagnetic in origin of equal range, low momentum central interaction to treat the charged hadronic systems. Since the effect due to charges becomes screened at a certain distance in real situations, we believe it desirable to include the effect of very short-range electromagnetic interaction. It is meant to point out that in such circumstances the effect of the combined potential is habitually inspected within the nuclear realm. We compute the scattering phase shifts and in turn the elastic cross sections via the variable phase approach for potential scattering to examine the merits of our constructed energy-dependent potentials over the earlier proposed central model by one of us. We present some model calculations in support of this.

KEY WORDS: Manning-Rosen plus Hulthén Potential, Regular solution, Supersymmetry transformation, Equivalent potentials, Phase shifts, Cross section

1 Introduction

For any quantum mechanical system exact analytical solutions of the wave equation are imperative as they provide all of the requisite information about the system under consideration. The Schrödinger equation can only be solved exactly for a few potentials like Coulomb, Square well, Harmonic oscillator, and r^{-4} type potentials in all partial waves and at all energies. The nuclear scattering of two charged hadrons generally occurs under the combined influence of two potentials, one is electromagnetic in nature, and the other is nuclear in origin. In the recent past, one of us (UL) [1, 2] advocated the problems containing nuclear Hulthén plus atomic Hulthén potential to treat the alpha-proton and alpha-alpha systems by calculating approximate higher partial wave solutions by exploiting ordinary differential equation approach together with the formalism of super-symmetric algebra. In the recent past, the same author (UL) proposed a new approximation scheme for hadronic systems [3, 4] and achieved good fit to nucleon-nucleon and nucleus-nucleus scattering observables with respect to on

and off-shell effects. The electromagnetic potential is in principle well known and is the longest-range part (infinite) of the interaction. But, in reality, this is not the case. In real situation the infinite long-range part of the interaction becomes screened at some distance. The main thought of scattering theory is that the colliding particles are assumed to move freely at large distances (we do not consider the Coulomb interaction). This asymptotic behavior is prearranged in the incoming and outgoing states. Thus, short-range electromagnetic potentials are applied to observe the effect of screening in describing the physical processes. In Ref. [3] an interaction model with equal range of both the nuclear and electromagnetic parts have been adapted to treat the nuclear systems.

Phase equivalent potentials have been constructed by several researchers [5–16] by exploiting the methodology of Supersymmetric (SUSY) Quantum Mechanics [17, 18] and variable phase approach [19]. It is well known that supersymmetric transformations are a commanding tool to manoeuvre the properties of the potential fields in quantum mechanics. For example, supersymmetric quantum mechanics allows the creation of potentials that are exactly solvable or that display exciting symmetry properties like shape invariance, or the manipulation of the discrete spectra of these potentials. These classical applications of supersymmetry are extremely enormous and are the subject of importance. A supersymmetric transformation for a given partial wave is a powerful tool to deal with its scattering properties because under such a transformation the scattering matrix is simply multiplied by a first-order rational function of the momentum. In nuclear physics both deep and shallow potentials have been studied to describe nucleus-nucleus interactions quite effectively. Within the framework of inverse scattering theory and the SUSY algebra, several authors [6, 8–12, 15] have studied the relation between shallow and deep potentials which are phase equivalent. In our previous article [20] we have developed phase equivalent potential by considering Manning-Rosen [21–24] one as the nuclear interaction and the electromagnetic part of the potential was added externally to treat charged systems. In the present work we rather concentrate on the use of SUSY transformations [5, 7] along with the conjecture used in Refs. [3] & [4]. The present article is an effort in this direction with Manning-Rosen plus Hulthén potential. The construction of phase equivalent energy-dependent interaction within the formalism of SUSY quantum mechanics requires the wave functions of the associated states. For a scattering problem, the Jost solutions $f_l(k, r)$ and $f_l(-k, r)$ which behave asymptotically as outgoing and incoming solutions respectively play a crucial role. The analytic continuation of the Jost solution in the upper half of the complex momentum plane reproduces the bound state wave function [25, 26]. As a basic input, we make use of the wave functions as developed by Sarkar et al. [3] to construct realistic energy-dependent potentials similar to the well-known phenomenological potentials. The main objective of this work is to judge the merits of these phase equivalent energy-dependent potentials over the central model of interactions of Ref. [3] by computing and

comparing the phase parameters of these interactions for nucleon-nucleon and nucleon-nucleus systems through the variable phase approach (VPA) [19]. The article is organized as follows. In Section 2 we briefly outline the methodology. Section 3 is devoted to results and discussion. We put our concluding remarks in Section 4.

2 Methodology

The Schrödinger equation for all partial waves with the combined potential $V_{l\,\mathrm{com}}(r)$ is given by

$$\left[\frac{d^2}{dr^2} + k^2 - V_{l\,\mathrm{com}}(r)\right]\psi_l(k,r) = 0\,, \tag{1}$$

where the potential $V_{l\,\mathrm{com}}(r)$ is assumed to be spherically symmetric and multiplied by $\frac{2\mu}{\hbar^2}$. Here the combined potential

$$V_{l\,\mathrm{com}}(r) = V_{lm}(r) + V_H(r)\,, \tag{2}$$

where $V_{lm}(r)$ stands for Manning-Rosen potential, which constitutes the nuclear part of the interaction and $V_H(r)$ is the atomic Hulthén potential, representing the electromagnetic part of the interaction. The quantity k is the centre of mass momentum of the system. The Manning-Rosen and Hulthén potentials read as

$$V_{lm}(r) = b^{-2}\left[\frac{\alpha(\alpha-1)e^{-2r/b}}{(1-e^{-r/b})^2} + \frac{l(l+1)e^{-2r/b}}{(1-e^{-r/b})^2} - A\frac{e^{-r/b}}{1-e^{-r/b}}\right] \tag{3}$$

and

$$V_H(r) = V_0\frac{e^{-r/a}}{1-e^{-r/a}}\,, \tag{4}$$

respectively. The parameters A and α, of the Manning-Rosen potential are dimensionless while the parameter b has a dimension of length. For the Hulthén potential, V_0 and a represent the strength and screening radius while the product $V_0\ a$ is equal to $2k\eta$ (η is the Sommerfeld parameter). For simplicity of calculation, we consider same range parameters for both the nuclear and electromagnetic parts of the interactions. Here we proceed with $a = b$. Hence, Eq. (1) together with Eqs. (3) and (4) yields

$$\left[\frac{d^2}{dr^2} + k^2 - b^{-2}\left[\frac{\alpha(\alpha-1)e^{-2r/b}}{(1-e^{-r/b})^2} + \frac{l(l+1)e^{-2r/b}}{(1-e^{-r/b})^2} - (A - V_0b^2)\frac{e^{-r/b}}{1-e^{-r/b}}\right]\right]\psi_l(k,r) = 0\,. \tag{5}$$

The irregular/Jost solution corresponding to above equation is given by [3]

$$f_l(k,r) = (1-e^{-\frac{r}{b}})^{-p}e^{ikr} \times {}_2F_1(1-a'^*, 1-b'^*; 1-2ikb; e^{-\frac{r}{b}})\,, \tag{6}$$

where

$$p = \frac{1}{2}\left[1 \pm \sqrt{1 + 4\alpha(\alpha - 1) + (l(l+1))}\right] - 1, \tag{7}$$

$$a' = 1 + p - ikb + (p^2 - k^2b^2 + p + A - V_0A)^{\frac{1}{2}} \tag{8}$$

and

$$b' = 1 + p - ikb - (p^2 - k^2b^2 + p + A - V_0A)^{\frac{1}{2}}. \tag{9}$$

In SUSY quantum mechanics any Hamiltonian H which has a ground state $({\psi_n}^{(0)}, {E_0}^{(0)})$ can be factorized as: $H = O_n^{(+)}O_n^{(-)} + E_0^{(0)}$, with

$$O_n^{\pm} = \frac{1}{\sqrt{2}}\left(\pm\frac{d}{dr} + \frac{d}{dr}\ln\psi_n^0(r, {E_0}^{(0)})\right); \quad n = 1, 2... \tag{10}$$

Using these lowering $O_n^{(+)}$ and raising $O_n^{(-)}$ operators, supersymmetric partner Hamiltonian is obtained as

$$\begin{aligned}\tilde{H} &= {E_0}^{(0)} + O_n^-({E_0}^{(0)})O_n^+({E_0}^{(0)}) \\ &= H + [O_n^-(E^{(0)}), O_n^+(E^{(0)})]\,,\end{aligned} \tag{11}$$

where $\tilde{H}$ has identical spectral lines to H except for the missing ground state. Similarly, one can introduce other higher "supersymmetric partner" Hamiltonians by iterating the process leading to Eqs. (10) and (11). Considering this to be the basis of the first transformation T_1, we conclude that T_1 removes the bound state at any arbitrary energy of a given Hamiltonian while maintaining the rest of the spectrum unaltered, as described by Sukumar [5, 7]. With similar mathematical manipulation, several bound states below the existing ground state can be added, which is denoted by the SUSY transformation T_2. The other two transformations T_3 and T_4 keep the spectrum intact with some alteration of the Jost function. Mathematically, when the transformations are applied successively in pairs of two, sixteen possible combinations of transformations are obtained, out of which three pairs are identical as they yield the same outcomes $(T_iT_j = T_jT_i)$. The order of the transformation does not change the end results. The potential form that one gets after the T_1 transformation is

$$V_{l1}(r) = V_{l\,\mathrm{com}}(r) - \frac{d^2}{dr^2}\ln{\psi_l}^{(0)}(r)\,, \tag{12}$$

where $\psi_l^{(0)}(r)$ stands for the near the origin behaviour of the ground state wave function. The corresponding wave function for $V_{l1}(r)$ reads as

$$\tilde{\Psi}_{l1}(r, E^0, \lambda) = \frac{1 + \lambda\int_0^r({\psi_l}^{(0)}(x))^2dx}{({\psi_l}^{(0)}(r))}; \quad -1 < \lambda < \infty. \tag{13}$$

As the T_2 transformation has the ability to add an additional bound state below the existing ground state of potential $V_{l1}(r)$ in Eq. (12), a combined effect of

T_1T_2 transformations keeps the whole spectrum unaltered and thus one obtains a phase equivalent potential with modified normalization constant. The transformed potential yields [5]

$$V_{l12}(k,r) = V_{l\,\mathrm{com}}(r) - \frac{d^2}{dr^2}\ln\tilde{\psi_{l1}}(r,E^0,\lambda)$$
$$= V_{l\,\mathrm{com}}(r) - \frac{d^2}{dr^2}\ln\left(1+\lambda\int_0^r(\psi_l^{(0)}(x))^2dx\right). \quad (14)$$

Here, the quantity λ is an adjustable parameter to be fitted to reproduce correct phase shifts with the energy-dependent potentials. When the transformation T_1 is operated followed by T_3, the new potential arrives at

$$V_{l13}(k,r) = V_{l\,\mathrm{com}}(r) - \frac{d^2}{dr^2}\ln\left(\int_0^r(\psi_l^{(0)}(x)^2)dx\right). \quad (15)$$

The potential $V_{l13}(k,r)$ is phase equivalent to $V_{l12}(k,r)$ except the ground state is missing. Similarly, the transformations T_2T_4 lead to another phase equivalent potential which reads as

$$V_{l24}(k,r) = V_{l\,\mathrm{com}}(r) - \frac{d^2}{dr^2}\ln\left(1+\int_r^\infty(f_l(k,x))^2dx\right). \quad (16)$$

The irregular/Jost solution plays a very crucial role in quantum scattering theory. Near the origin behaviour of the Jost solution $f_l(k,r)$ reproduces the Jost function $f_l(k)$ according to the relation [25,26]

$$f_l(k) = \lim_{r\to 0}(kr)^l\frac{e^{(-il\pi/2)}}{(2l+1)!!}f_l(k,r).$$

If $f_l(k,r)$ is decreasing exponentially at infinity for $\mathrm{Im}\,k > 0$, then one gets a regular square-integrable wave function and consequently an eigenvalue. Therefore, the Jost solution for $\mathrm{Im}\,k > 0$ reproduces the bound-state wave function and zeros of the Jost function give the bound-state energies [25, 26]. To derive the analytical expressions for energy-dependent potentials in Eqs. (12) and (14)–(15) one requires the bound state wave functions of the concerned parent potential. To that end, we put $k = i\omega$ in Eq. (6) together with the following transformation [27,28]:

$${}_2F_1(a,b,c,z) = (1-z)^{c-a-b}\,{}_2F_1(c-a,c-b,c,z) \quad (17)$$

to get

$$\psi_l(r) = (1-e^{-r/b})^{-p}e^{-\omega r}(1-e^{-r/b})^{4\omega b+2p-1}$$
$$\times\,{}_2F_1(2\omega b+a'^*,2\omega b+b'^*,1+2\omega b;e^{-r/b}) \quad (18)$$

To derive the analytical expressions for phase equivalent potentials $V_{l1n}(k,r)$; $n=2,3$ in Eqs. (14) and (15) one needs the knowledge of $\psi_l^{(0)}(r)$ which defines near the origin behavior of the bound state wave function [8, 12, 13, 29]. Thus, $\psi_l^{(0)}(r)$ reads as

$$\psi_l^{(0)}(r) = (1-e^{-r/b})^{4\omega b+p+1} e^{-\omega r}. \tag{19}$$

For the calculation of $V_{l24}(k,r)$, the irregular solution Eq. (6) is used to solve Eq. (16). Using $\psi_l^{(0)}(r)$ in Eqs. (14) and (15) and $f_l(k,r)$ in Eq. (16) along with the transformation [30]

$$\int_0^u \frac{x^{\mu-1}}{(1+\beta x)^\gamma} dx = \frac{u^\mu}{\mu} {}_2F_1(\gamma,\mu;1+\mu;-\beta u)\,, \tag{20}$$

$$\begin{aligned} V_{l12}(k,r) &= V_{l\,\mathrm{com}}(r) - \frac{d^2}{dr^2}\ln(1+\lambda\frac{(1-e^{-r/b})^{8\omega b+2p-1}}{8\omega b+2p-1} \\ &\times {}_2F_1(-2\omega b, 8\omega b+2p-1; 8\omega b+2p; 1-e^{(-r/b)})) \\ &= V_{l\,\mathrm{com}}(r) - \left(\frac{P''}{P} - \left(\frac{P'}{P}\right)^2\right), \end{aligned} \tag{21}$$

$$\begin{aligned} V_{l13}(k,r) &= V_{l\,\mathrm{com}}(r) - \frac{d^2}{dr^2} ln(\frac{(1-e^{-r/b})^{8\omega b+2p-1}}{8\omega b+2p-1} \\ &\times {}_2F_1(-2\omega b, 8\omega b+2p-1; 8\omega b+2p; 1-e^{(-r/b)})) \\ &= V_{l\,\mathrm{com}}(r) - \left(\frac{R''}{R} - \left(\frac{R'}{R}\right)^2\right), \end{aligned} \tag{22}$$

$$V_{l24}(k,r) = V_{l\,\mathrm{com}}(r) - \left(\frac{S''}{S} - \left(\frac{S'}{S}\right)^2\right) \tag{23}$$

with

$$\begin{aligned} P &= 1+\lambda\frac{(1-e^{-r/b})^{8\omega b+2p-1}}{8\omega b+2p-1} \\ &\times {}_2F_1(-2\omega b, 8\omega b+2p-1; 8\omega b+2p; 1-e^{(-r/b)}) \end{aligned} \tag{24}$$

$$\begin{aligned} R &= \frac{(1-e^{-r/b})^{8\omega b+2p-1}}{8\omega b+2p-1} \\ &\times {}_2F_1(-2\omega b, 8\omega b+2p-1; 8\omega b+2p; 1-e^{(-r/b)}) \end{aligned} \tag{25}$$

and

$$\begin{aligned} S = 1 + \frac{z^C}{C}F_a + \frac{2ABz^{C+1}}{C(C+1)}F_b + \Big(\frac{AB(A+1)(B+1)}{C(C+1)} + \frac{(AB)^2}{C^2}\Big) \\ \times \frac{z^{C+2}}{C+2}F_c + \frac{(AB)^2(A+1)(B+1)}{C^2(C+1)}\frac{z^{(C+3)}}{C+3}F_d\,, \end{aligned} \tag{26}$$

where $z = e^{-r/b}$; $A = 1 - a'^{*}$; $B = 1 - b'^{*}$; $C = -2ikb$ and

$$F_a = {}_2F_1(2p, C; C+1; z)\,; \qquad F_b = {}_2F_1(2p, C; C+2; z)\,;$$
$$F_c = {}_2F_1(2p, C; C+3; z)\,; \qquad F_d = {}_2F_1(2p, C; C+4; z)$$

are used as notations to abbreviate the equation. The quantities P', P", R', R", S and S" are the first and second derivatives of P, R and S with respect to r. The phase shifts for the potentials in Eqs. (21)–(23) can easily be calculated by solving the following nonlinear differential equation [19]:

$$\delta_l'(k,r) = -k^{-1}V(k,r)\left[\cos\delta_l(k,r)\hat{J}_l(kr) - \sin\delta_l(k,r)\hat{\omega}_l(kr)\right]^2 . \quad (27)$$

This equation is solved numerically from origin to asymptotic region to get the required phase shift $\delta_l(k)$. The functions $\hat{j}_l(k,r)$ and $\hat{\omega}_l(k,r)$ represent the Riccati-Bessel functions.

3 Results and Discussion

The value of $\hbar^2/2\mu$ is taken to be 41.47 MeV fm^2 for p-p system and 25.92 MeV fm^2 for α-p system, where μ is the reduced mass. The parameter λ is taken to be 0.001 to have the best fit of the phase parameters with standard data. The product $V_0 b$ (equal to $2k\eta$) takes the values 0.03472 fm^{-1} and 0.1117 fm^{-1} for p-p and α-p system respectively.

We have fixed the parameters of different states for both p-p and α-p systems by giving free running to our parameters in the numerical routine to reproduce reliable phase parameters [15,30–36]. Using the parameters listed in Table 1 for different phase equivalent potentials, the scattering phase shifts are presented graphically with reference data [31,33–35] in Figures 1–5. A close observation of the graphs 1–5 suggests that our results generate correct trends of phase shifts

Table 1. Parameters of Manning-Rosen potential for p-p and α-p systems

System	State	A	b (fm)	α
p-p	$^1S_0$	0.952	1.152	-0.0043
	$^3P_0$	1.32	1.1	0.005
	$^3P_2$	0.75	1.01	0.005
	$^1D_2$	1.05	1.22	0.72
α-p	$1/2(+)$	2.35	1.215	0.005
	$1/2(-)$	3.66	1.20	0.005
	$3/2(-)$	5.72	1.03	0.005
	$3/2(+)$	2.535	1.03	0.005
	$5/2(+)$	2.95	1.03	0.005

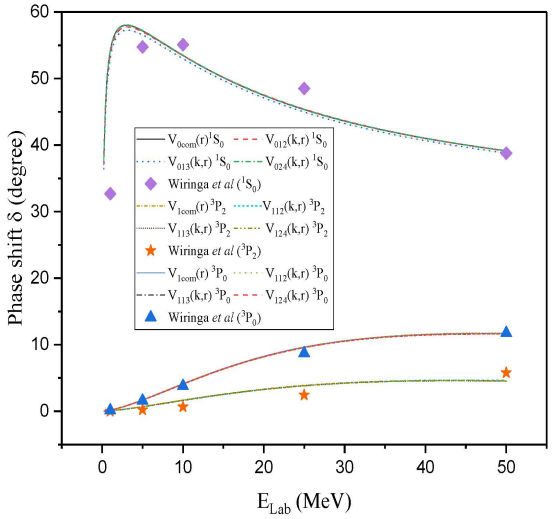

Figure 1. Scattering phase shifts for p-p ${}^1S_0$, ${}^3P_0$ and ${}^3P_2$ states with standard data.

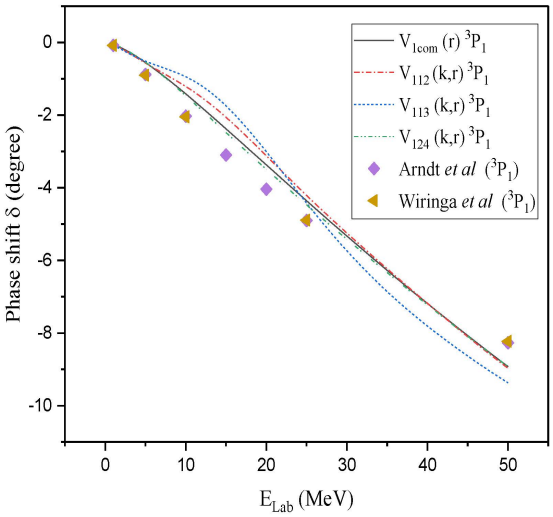

Figure 2. Scattering phase shifts for p-p ${}^3P_1$ state with standard data.

for $l = 0, 1$ and 2 partial waves with the phase equivalent potentials $V_{l12}(k, r)$, $V_{l13}(k, r)$ and $V_{l24}(k, r)$.

Figure 1, depicting the ${}^1S_0$, ${}^3P_2$ and ${}^3P_0$ p-p phase shifts, clearly shows that both ${}^3P_2$ and ${}^3P_0$ phase shifts follow a similar trend with a quantitative disagreement of $0.5^0 - 2^0$ with those of Wiringa et al. [33]. The ${}^1S_0$ phase peak

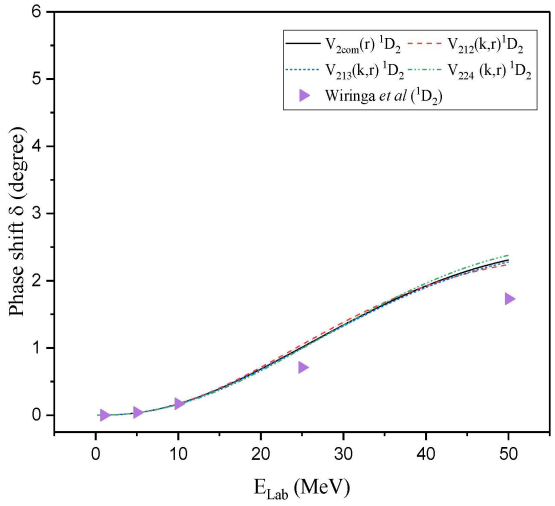

Figure 3. Scattering Phase shifts for p-p ${}^1D_2$ state with standard data.

value of our computed phase shifts at $E_{\text{Lab}} = 3$ MeV is slightly higher (2.5^0) compared to the standard data (peak at 5 MeV) [33] while rest of the values match quite well. It is also noteworthy that all the phase equivalent potentials along with the original combined potential produce almost same phase shifts for the aforementioned states. Although, a slightly lower phase shifts are observer for $V_{013}(k,r)$ potential for ${}^1S_0$ p-p state, the difference is negligible. The ${}^3P_1$ state, with negative phase values as shown in Figure 2, agree qualitatively but disagree quantitatively with the standard results [33].

However, this disagreement in numerical values is within one degree. In Figure 3, it is noticed that the phase equivalent potentials produce a good match in the lower energy region (below 25 MeV). Beyond that some deviation from the standard data is observed. The observed differences in phase values are within one degree only. Figure 4 represents the scattering phase shifts of $1/2(+)$, $1/2(-)$ and $5/2(+)$ states for α-p system. The scattering phase shifts produced by phase equivalent potentials and the combined Manning-Rosen plus atomic Hulthén potential follow the trend of Satchler et al. [34] and Ali et al. [35]. The phase parameters for the $1/2(+)$ state show a continuous decreasing trend in agreement with the standard results [34, 35]. Though in the lower energy range, all the phase equivalent potentials as well as the combined Manning-Rosen and Hulthén potential produce significantly lower values of phase shifts, beyond 5 MeV while they reproduce Ref. [34] and Ref. [35] significantly well. Slight difference in phase shift values can be noticed between $V_{012}(k,r)$ $(1/2+)$ and $V_{024}(k,r)(1/2+)$ potentials where the former produces higher phase shifts than the latter. It is noticed, for $1/2(-)$ states, that the computed phase shifts match better with standard data [34, 35] in the high energy region (6–20 MeV), while

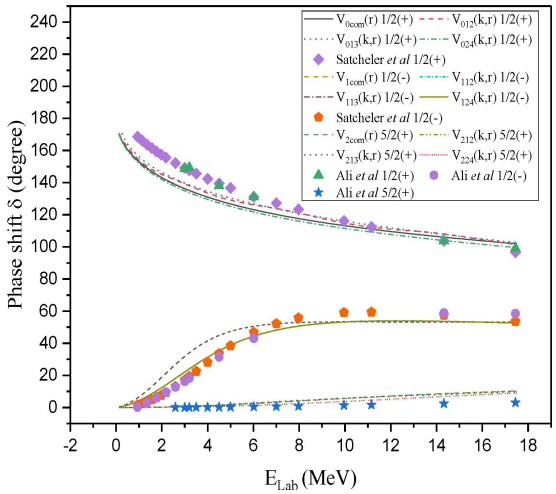

Figure 4. Scattering phase shifts for α-p $1/2(+)$, $1/2(-)$ and $5/2(+)$ states with standard data.

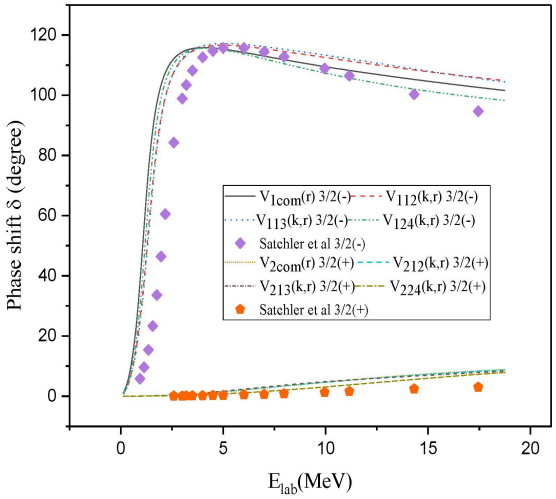

Figure 5. Scattering phase shifts for α-p $3/2(+)$ and $3/2(-)$ states with standard data.

there is slight mismatch in phase data in the low energy range for $V_{113}(k,r)$. The $5/2(+)$ phase shifts follow experimental data quite well. The α-p $3/2(-)$ phase shift data, shown in Figure 5, shows almost similar peak value as that of the standard data [34] with a lateral shift within the energy range 0–3 MeV. Beyond 5 MeV our results for $V_{112}(k,r)$ and $V_{113}(k,r)$ are slightly higher compared to the standard data but shows similar trend, where as $V_{124}(k,r)$ match better with

reference data. The $3/2(+)$ phase shifts in Figure 5 follow the same trend as that of $5/2(+)$ with a deviation of 2.5 degrees maximum which is within the permissible limit. The overall observation from the graphs suggests that the α-p phase shifts for higher partial waves have a better match with the standard data. From the foregoing inspection it is established that our constructed potentials are truly phase equivalent.

The ^{5}Li is an unbound system and all the information about this nucleus can be obtained from nuclear reaction processes. Our constructed Hamiltonian for α-p system only contains nucleon-nucleus plus electromagnetic central potentials barring any spin orbit or tensor interactions. The α-n and α-p phase shifts calculated by Quaglioni-Navrátil [37] and Forssén et al. [38] using the resonating group method and a microscopic description of the nuclear clusters with more realistic N3LO and CD-Bonn NN potentials achieved excellent S-wave phase shifts whereas for P-waves the same have insufficient magnitude with respect to experimental results. Our $1/2(-)$ phase shifts for α-p systems have a much better match with the Ref. [34] while the same for $3/2(-)$ state discern from those of experimental data [34] beyond 3.0 MeV maintaining the correct trend. Therefore, our potential models reproduce improved results than Refs. [36] and [37]. It is well established that the Coulomb interaction has a dominant role in case of charged hadron scattering at low energies which is reconfirmed by the slightly lower $1/2(+)$ scattering phase values for the α-p system. This discrepancy in phase parameters may be attributed to the fact that our model potentials are unable to account for the actual forces in experimentation in the very low energy range.

The effective-range expansion is the first step for the parameterization of nucleon–nucleon scattering. The purpose of this expansion is to find the values of the scattering length and effective range. The knowledge of these parameters also acts as a constructive tool for other nuclear systems. For example, in astrophysical applications the knowledge of the scattering length plays an important role in describing the low energy reactions [39]. In ^{5}Li nucleus the ground and first excited states are resonance states, which can be treated in single-channel p-α system. There is a narrow resonance in the p-α system for $J = 3/2$ while a wide resonance for $J = 1/2$. The $3/2(-)$ state is the ground state and $1/2(-)$ is the first excited state. Using the relation of the binding energy obtained from the zeros of the Jost function [3] we get $E_B = 1.514$ MeV and $E_B = 2.6296$ MeV for $3/2(-)$ and $1/2(-)$ states which are in conformity with the standard results [40] $E_B = 1.481$ MeV and $E_B = 2.611$ MeV respectively. To estimate the low energy scattering parameters, scattering length (fm) and the effective range (fm), the modified effective range formulation [41–43] is exploited to have $a_{(3/2-)} = 43.65$, $a_{(1/2-)} = -17.32$, $r_{(3/2-)} = -0.392$ and $r_{(1/2-)} = -0.073$ respectively.

As we are concerned here with low and intermediate energy scattering, the study of p-p resonances go beyond the scope of this article. The scattering cross sec-

tion is an effective area that enumerates the essential rate a given incident occurs during the scattering of two particle group. In the literature a large number of reliable low energy p-p and α-p parameter calculations [31–38] exists for various nucleon-nucleon interaction models. In view of small discrepancies between the results of these phase shift analysis and of our calculations, we desire to explore to what degree our model calculations will be able to yield realistic cross section data. A large amount of cross section data exists for p-p and α-p systems [43–49] with different nuclear force models. We analyze total scattering cross sections for the systems under consideration and compare them with the available data [43–47] in the literature. The same for α-p is portrayed in Figure 8 together with the experimental results of Brockman [47].

Arndt et al. [44, 45] determined total p-p cross section in the energy range 25 to 1000 MeV on the basis of recent energy-dependent fits and associated single-energy solutions. It is noticed that the elastic cross sections for p-p scattering (Figure 6) at low and intermediate energy region show symmetric nature about the central region of angles (around 90°) with shallow interference minima on both sides. It is demonstrated that around 90° the scattering is mainly due to the nuclear forces. Our results for differential scattering cross section at $E_{\text{Lab}} = 2.4$ MeV are in conformity with the observation of Jackson and Blatt [43]. At $E_{\text{Lab}} = 9.918$ MeV the p-p cross section resembles the character of both "discriminator scattering data (or D data)" and "background subtraction scattering data (BGS data)" up to the available experimental differential cross

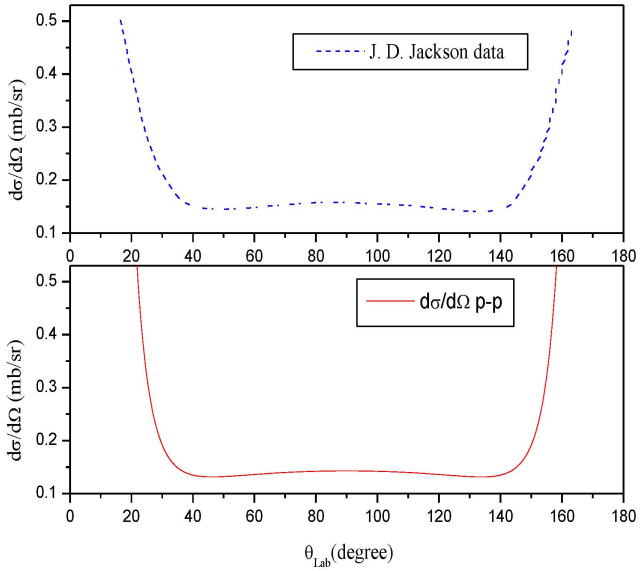

Figure 6. p-p elastic cross section for $E_{\text{Lab}} = 2.4$ MeV.

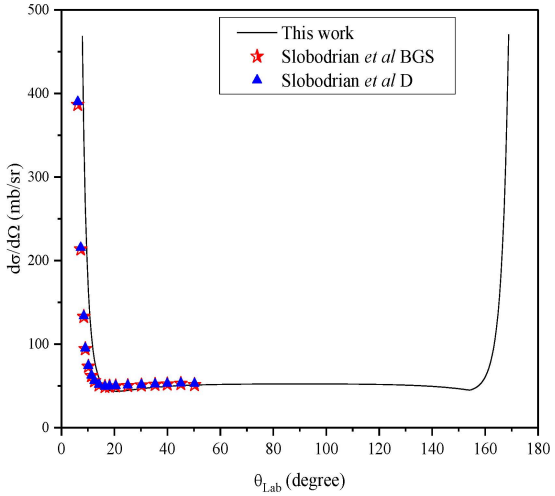

Figure 7. p-p elastic cross section for $E_{\mathrm{Lab}} = 9.918$ MeV. Experimental data are from Ref. [46].

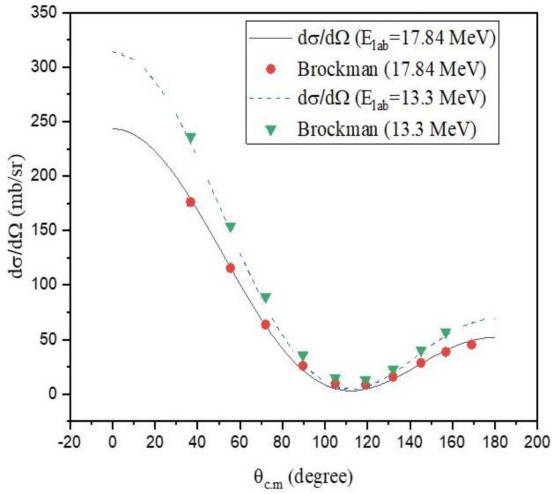

Figure 8. α-p elastic cross section for $E_{\mathrm{Lab}} = 13.3$ MeV and 17.84 MeV. Experimental data are from Ref. [47].

section data of 50 degrees as described in Slobodrian et al. [46], with a slight lateral shift at lower degrees. Our results for α-p system, are in close agreement with the experimental data of Brockman [47]. We have verified that both of our phase parameters for energy-independent and dependent potentials reproduce same cross sections.

The potentials are plotted against scattering radius in Figures 9–17, to study the natures of our constructed phase equivalent energy-dependent potentials along with the parent potential for both p-p and α-p systems for different partial waves $l = 0, 1$ and 2. The potentials are plotted in MeV by multiplying them with $\hbar^2/2\mu$ of the respective systems.

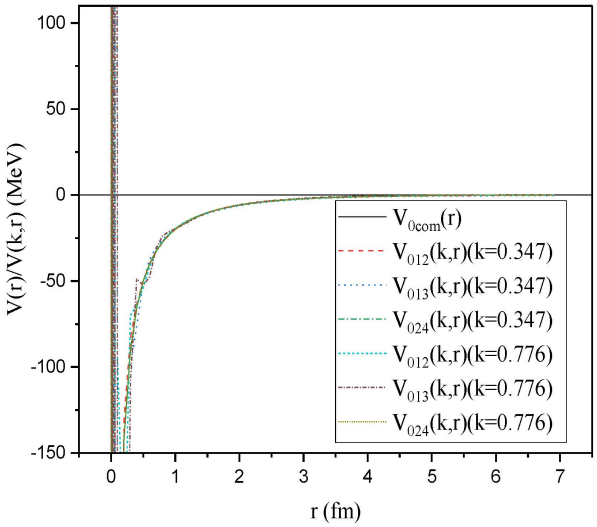

Figure 9. Potential plot for ${}^1S_0$ p-p state.

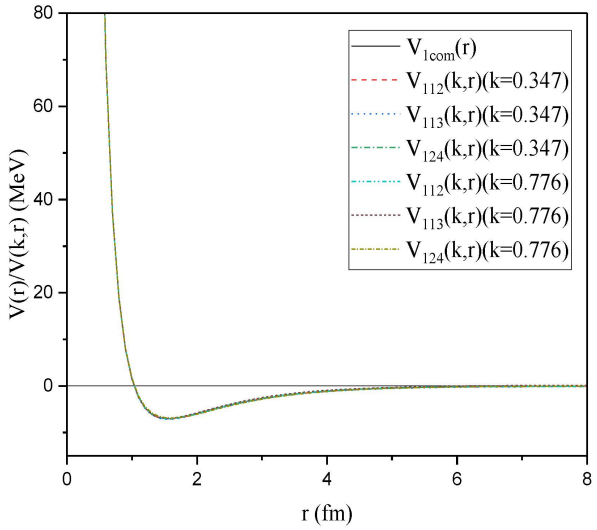

Figure 10. Potential plot for ${}^3P_0$ p-p state.

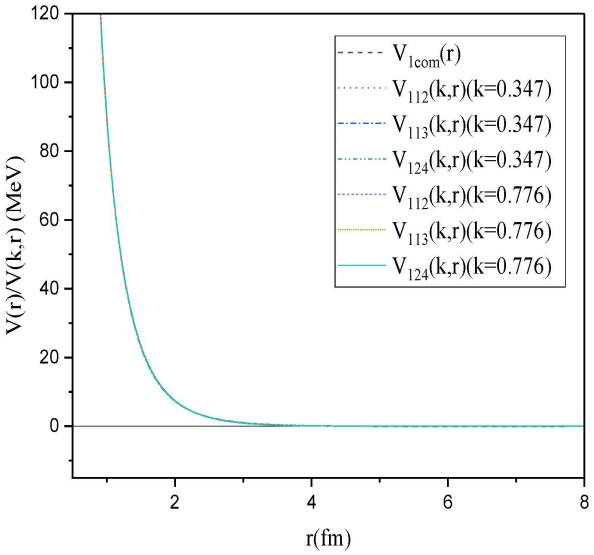

Figure 11. Potential plot for $^3P_1$ p-p state.

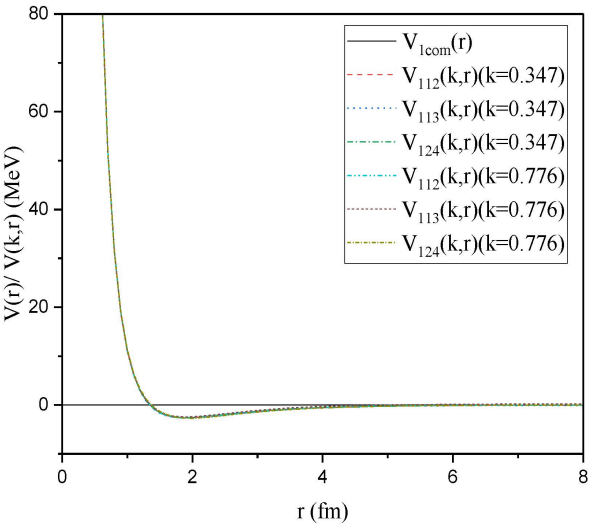

Figure 12. Potential plot for $^3P_2$ p-p state.

To verify the energy dependence the constructed potentials are portrayed for two different laboratory energies namely, $E_{\text{Lab}} = 5$ MeV ($k = 0.347$) and $E_{\text{Lab}} = 25$ MeV ($k = 0.776$) for p-p system whereas for α-p system, the energies are $E_{\text{Lab}} = 5$ MeV ($k = 0.439$) and $E_{\text{Lab}} = 20$ MeV ($k = 0.878$). From

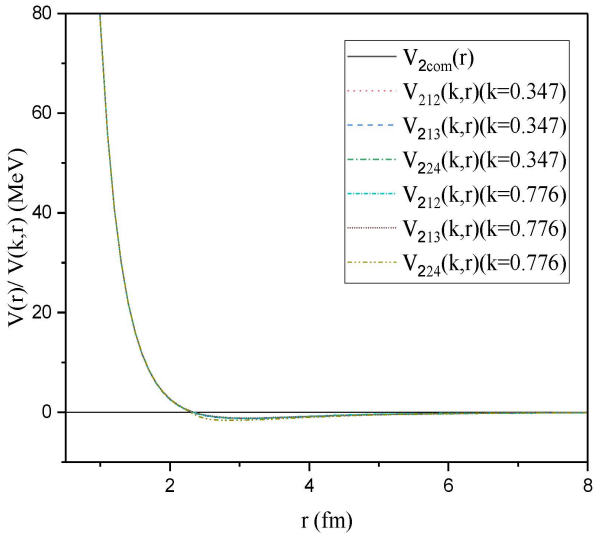

Figure 13. Potential plot for ${}^1D_2$ p-p state.

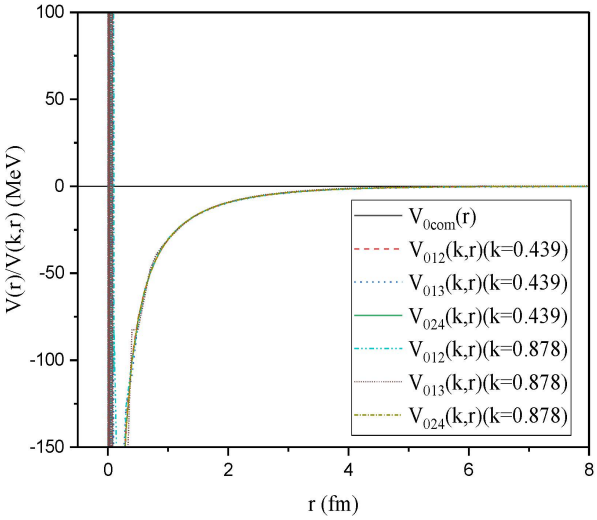

Figure 14. Potential plot of α-p 1/2(+) state.

the graphs, Figures 9–17, it is understood that the constructed phase equivalent potentials have weak energy dependence as they resemble $V_{l\,\mathrm{com}}$. The differences in strengths of the various energy-dependent potentials for a particular angular momentum state are too small to be detected in the scale of the figures. The observation made by Baye [6] about the strong energy dependence of phase

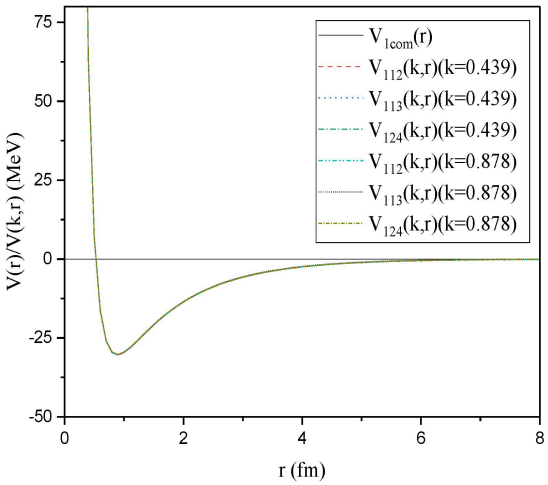

Figure 15. Potential plot of α-p 1/2(-) state.

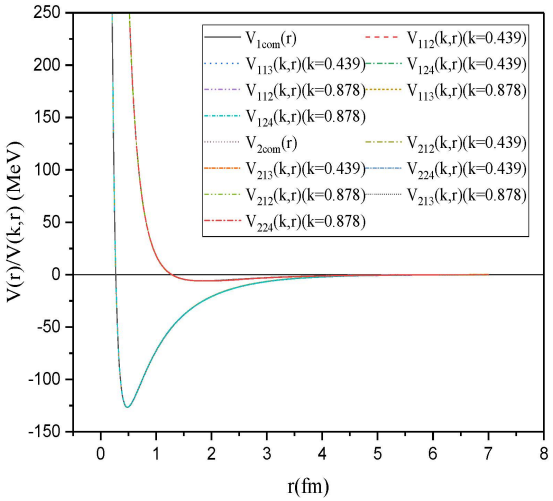

Figure 16. Potential plot of α-p 3/2(-) and 3/2(+) state.

equivalent potentials is not observed here. For both the hadronic systems under consideration, strong repulsive cores develop in the potentials due to electromagnetic and centrifugal barrier terms. It is well known that the Hulthén potential behaves as Coulomb potential for large screening radius or for small values of r. In Figure 18 we plot both these potentials with the parameters of α-p 1/2(+) state in support of this.

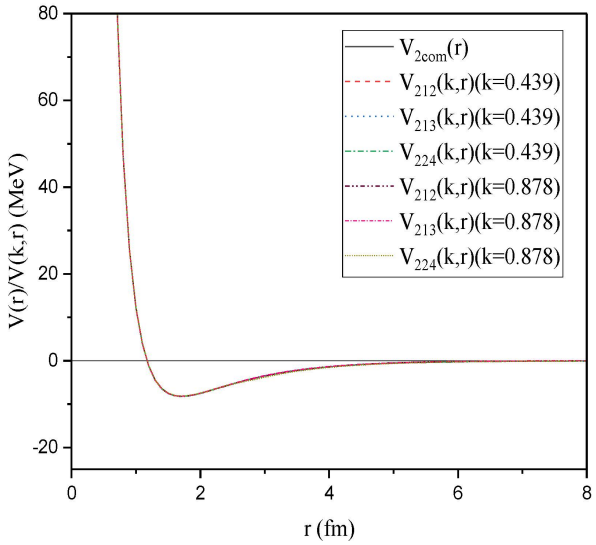

Figure 17. Potential plot of α-p 5/2(+) state.

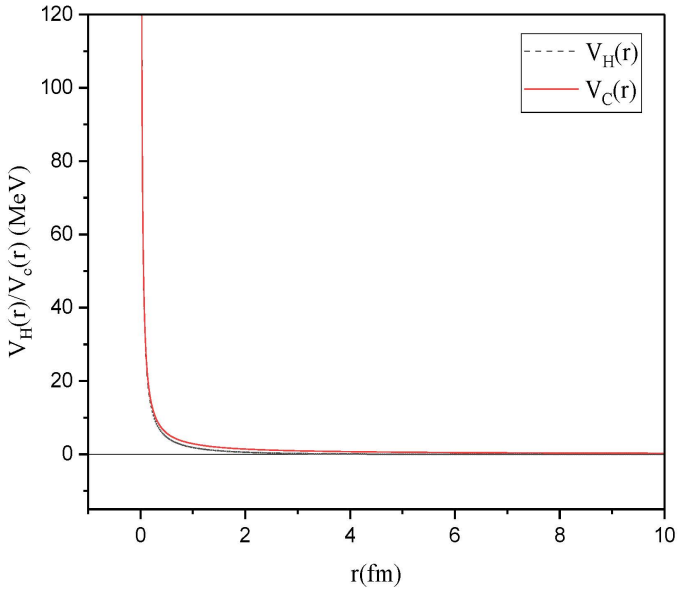

Figure 18. Comparison of the Coulomb and the Hulthén potentials.

4 Conclusion

In our previous work [20], we studied the charged hadron interaction by incorporating the electromagnetic interaction externally. In the present paper we propose a combined potential, electromagnetic plus nuclear in origin, to study low energy elastic scattering. The success of a phenomenological potential model depends on the reproduction of low energy scattering parameters up to partial waves $l \leq 3$. Our proposed central potential model and their energy dependent counter parts reproduced reliable low energy phase parameters, cross sections etc. and thus the name low momentum nuclear potential is justified. It is noticed that in certain cases our energy-dependent potentials namely $V_{l24}(k,r)$ and $V_{l13}(k,r)$ interactions for p-p system produce improved results than their central counterpart. The same argument is applicable for $V_{l12}(k,r)$ in case of $\alpha - p$ system. In this work we have not included spin-orbit coupling or tensor interactions to our central potential. The ^{5}Li is an unbound system with narrow P-wave resonances in the $3/2(-)$ and $1/2(-)$ channels whose binding energies, scattering lengths and effective ranges have been reproduced quite effectively by our model potential. The overall agreement between the theoretical and experimental data, with respect to scattering parameters and cross sections, is quite remarkable. We conclude that our constructed energy-dependent potentials are fundamentally equivalent to energy-independent counterpart. It is anticipated that with the inclusion of spin-orbit interaction the low energy discrepancies in α-p $1/2(+)$ phase shifts may be remedied. The topic of this work has been the investigation of the effect of the very short range (equal to nuclear one) electromagnetic interaction in charged hadron scattering and found it quite successful.

References

[1] J Bhoi, U Laha (2017) Supersymmetry-inspired low-energy α–p elastic scattering phases. *Theor. Math. Phys.* **190** 69-76.

[2] U. Laha, M Majumder, J. Bhoi (2018) Volterra integral equation-factorisation method and nucleus–nucleus elastic scattering. *Pramana - J. Phys.* **90** 1-7.

[3] P. Sarkar, B. Khirali, U. Laha, P. Sahoo (2021) Exact solution of two-potential system under same range approximation and its implication. *Int. J. Mod. Phys. E* **30** 2150066.

[4] P. Sahoo, U. Laha (2022) Treatment of hadronic systems involving two potentials under a new approximation scheme. *Pramana - J. Phys.* **96** 15-20.

[5] C.V. Sukumar (1985) Supersymmetric quantum mechanics of one-dimensional systems. *J. Phys. A: Math. Gen.* **18** 2917.

[6] D. Baye (1987) Supersymmetry between deep and shallow nucleus-nucleus potentials. *Phys. Rev. Lett.* **58** 2738-2741.

[7] C.V. Sukumar (1985) Supersymmetric quantum mechanics and the inverse scattering method. *J. Phys. A: Math. Gen.* **18** 2937.

[8] U. Laha, C. Bhattacharyya, K. Roy, B. Talukdar (1988) Hamiltonian hierarchy and the Hulthén potential. *Phys. Rev. C* **38** 558.

[9] A. Khare, U. Sukhatme (1989) Phase-equivalent potentials obtained from supersymmetry. *J. Phys. A: Math. Gen.* **22** 2847.

[10] B. Talukdar, U. Das, C. Bhattacharyya, P.K. Bera (1992) Phase-equivalent potentials from supersymmetric quantum mechanics. *J. Phys. A: Math. Gen.* **25** 4073.

[11] U. Laha, J. Bhoi (2013) On the nucleon–nucleon scattering phase shifts through supersymmetry and factorization. *Pramana - J. Phys.* **81** 959-973.

[12] J. Bhoi, U. Laha (2013) Hamiltonian hierarchy and n–p scattering. *J. Phys. G Nucl. Part. Phys.* **40** 045107.

[13] J. Bhoi, U. Laha, K. C. Panda (2014) Nucleon–nucleon scattering in the light of supersymmetric quantum mechanics. *Pramana - J. Phys.* **82** 859–865.

[14] J. Bhoi, U. Laha (2017) Hulthén potential models for $\alpha - \alpha$ and $\alpha -^3$ He elastic scattering. *Pramana - J. Phys.* **88** 1-6.

[15] U. Laha, J. Bhoi (2015) Higher partial-wave potentials from supersymmetry-inspired factorization and nucleon-nucleus elastic scattering. *Phys. Rev. C* **91** 034614.

[16] J. Bhoi, U. Laha (2015) Supersymmetry-generated jost functions and nucleon–nucleon scattering phase shifts. *Phys. Atom. Nucl.* **78** 831–834.

[17] E. Witten (1981) Dynamical breaking of supersymmetry. *Nucl. Phys. B* **188** 513–554.

[18] F. Cooper, B. Freedman (1983) Aspects of supersymmetric quantum mechanics. *Ann. Phys.* **146** 262–288.

[19] F. Calogero (1967) "*Variable Phase Approach to Potential Scattering*". Academic Press, New York.

[20] M. Majumder, U. Laha (2022) Phase-equivalent potentials using SUSY transformations. *Pramana - J. Phys.* **96**(3) .

[21] M.F. Manning, N. Rosen (1933) A potential function for the vibrations of diatomic molecules. *Phys. Rev.* **44**(11) 951–954.

[22] B. Khirali, A.K. Behera, J. Bhoi, U. Laha (2019) Regular and jost states for thes-wave manning–rosen potential. *J. Phys. G Nucl. Part. Phys.* **46** 115104.

[23] S.-H. Dong, J. Garcia-Ravelo (2007) Exact solutions of the s-wave Schrodinger equation with manning–rosen potential. *Phys. Scr.* **75**(3) 307.

[24] B. Khirali, A.K. Behera, J. Bhoi, U. Laha (2020) Scattering with Manning–Rosen potential in all partial waves. *Ann. Phys.* **412** 168044.

[25] R.G. Newton (2013) "*Scattering theory of waves and particles*". Springer Science and Business Media, New York.

[26] S. Adhikari (2012) "*Dynamical collision theory and its applications*". Academic Press.

[27] A. Erdélyi, W. Magnus, F. Oberhettinger, F. Tricomi (1953) "*Higher transcendental functions*". McGraw-Hill, New York.

[28] L.J. Slater (1966) "*Generalized hypergeometric functions*". Cambridge University Press, London.

[29] U. Laha, C. Bhattacharyya, B. Talukdar (1986) Ladder operator relations for hypergeometric functions. *J. Phys. A: Math. Gen.* **19**(9) L473.

[30] I.S. Gradshteyn, I.M. Ryzhik (2014) "*Table of integrals, series, and products*". Academic press, New York.

[31] R.A. Arndt, L.D. Roper, R.A. Bryan, R.B. Clark, B.J. VerWest, P. Signell (1983) Nucleon-nucleon partial-wave analysis to 1 gev. *Phys. Rev. D* **28** 97-122.

[32] R.J. Bystricky, C. Lechanoine (1987) Nucleon-nucleon phase shift analysis . *Journal de Physique* **48** 199-226.

[33] R.B. Wiringa, V. Stoks, R. Schiavilla (1995) Accurate nucleon-nucleon potential with charge-independence breaking. *Phys. Rev. C* **51** 38–51.

[34] G. Satchler, L. Owen, A. Elwyn, G. Morgan, R. Walter (1968) An optical model for the scattering of nucleons from 4he at energies below 20 mev. *Nucl. Phys. A* **112** 1-31.

[35] S Ali, A.A.Z. Ahmad, N. Ferdous (1985) A survey of the alpha-nucleon interaction. *Rev. Mod. Phys.* **57** 923-964.

[36] J. Dohet-Eraly, D. Baye (2011) Microscopic cluster model of $\alpha + n$, $\alpha + p$, $\alpha +$ ^{3}He, and $\alpha + \alpha$ elastic scattering from a realistic effective nuclear interaction. *Phys. Rev. C* **84**(1) 014604.

[37] S. Quaglioni, P. Navrátil (2009) Ab initio many-body calculations of nucleon-nucleus scattering. *Phys. Rev. C* **79**(4) 044606.

[38] C. Forssén, G. Hagen, M. Hjorth-Jensen, W. Nazarewicz, J. Rotureau (2013) Living on the edge of stability, the limits of the nuclear landscape. *Phys. Scr.* **2013** T152 014022.

[39] D. Baye (2000) Behavior of the 7 Be (p, γ) 8 B astrophysical S factor near zero energy. *Phys. Rev. C* **62**(6) 065803.

[40] Y.V. Orlov (2020) The energies and ANCs for 5Li resonances deduced from experimental p-α scattering phase shifts using the effective-range and Δ methods. *Nucl. Phys. A* **1004** 122060.

[41] J. Hamilton, I. Øverbö, B. Tromborg (1973) Coulomb corrections in non-relativistic scattering. *Nucl. Phys. B* **60** 443-477.

[42] H. Van Haeringen (1977) T matrix and effective range function for Coulomb plus rational separable potentials especially for I= 1. *J. Math. Phys.* **18**(5) 927–940.

[43] J.D. Jackson, J.M. Blatt (1950) The interpretation of low energy proton-proton scattering. *Rev. Mod. Phys.* **22**(1) 77-118.

[44] R.A. Arndt, J.S. Hyslop III, L.D. Roper (1947) Nucleon-nucleon partial-wave analysis to 1100 mev. *Phys. Rev. D* **35**(1) 128-144.

[45] R.A. Arndt, I. Strakovsky, R. Workman (2000) Nucleon-nucleon elastic scattering to 3 GeV. *Phys. Rev. C* **62** 034005.

[46] R. Slobodrian, H. Conzett, E. Shield, W. Tivol (1968) Proton-proton elastic scattering between 6 and 10 MeV. *Phys. Rev.* **174** 1122.

[47] K.W. Brockman (1957) Scattering of Protons by Helium between 11.4 Mev and 18 Mev. *Phys. Rev.* **108** 1000-1006.

[48] V. Comparat, R. Frascaria, N. Fujiwara, N. Marty, M. Morlet, P.G. Roos, A. Willis (1975) Elastic proton scattering on ^{4}He at 156 MeV. *Phys. Rev.* **12** 251-255.

[49] J. Berger, J. Duflo, L. Goldzahl, F. Plouin, J. Oostens, M. Van Den Bossche, L. Vu Hai, G. Bizard, C. Le Brun, F.L. Fabbri, P. Picozza, L. Satta (1976) Measurement of Medium Energy Alpha-Proton Elastic Scattering beyond the First Minimum Region. *Phys. Rev. Lett.* **37** 1195-1198.